5128 *Macromolecules* **2010**, *43*, 5128–5136
DOI: 10.1021/ma100400q

Macromolecules
ARTICLE

Phase Behavior of Nonfrustrated ABC Triblock Copolymers: Weak and Intermediate Segregation

Jian Qin, Frank S. Bates, and David C. Morse*

Department of Chemical Engineering and Materials Science, University of Minnesota, 421 Washington Ave. S.E., Minneapolis, Minnesota 55455

Received February 21, 2010; Revised Manuscript Received April 27, 2010

ABSTRACT: The phase behavior of ABC triblock copolymer melts is studied using weak segregation theory and numerical self-consistent field theory (SCFT). We focus on nonfrustrated systems, with interaction parameters $\chi_{AB} \simeq \chi_{BC} < \chi_{AC}$. Phase behavior of completely symmetric systems, with $\chi_{AB} = \chi_{BC}$ and equal A and C volume fractions, $f_A = f_C$, is studied over a range of values of $\chi_{AC}N$ and the ratio $k \equiv \chi_{AC}/\chi_{AB}$, in order to resolve some qualitative differences between the results of previous SCFT studies that were carried out at very different values of k. Studies of full composition triangles are presented for two models with parameters similar to those of poly(isoprene-styrene-ethylene oxide), using values of $\chi_{ij}N$ twice those used in our previous study of the same models. A stable alternating diamond phase, with interpenetrating A and C diamond networks, is found to be stable in symmetric systems in a small region near the ODT. The *Fddd* (O^{70}) phase of slightly asymmetric ABC triblocks is shown to remain stable well into the intermediate segregation regime.

I. Introduction

While the self-consistent field theory (SCFT) of diblock copolymer melts is well established, understanding of multiblock copolymer architectures remains much less mature. Several groups have now used different variants of SCFT[1−11] to study limited regions of the large parameter space of ABC triblock copolymers. We focus here, as in our own previous theoretical work[8,9] on so-called "nonfrustrated" ABC triblocks, in which the Flory−Huggins parameter χ_{AC} associated with the interaction between the end blocks is larger than parameters χ_{AB} and χ_{BC} between middle and end blocks, and in which $\chi_{AB} \simeq \chi_{BC}$.

The present study extends and unifies several previous theoretical studies of this class of systems by Matsen,[5] Erukhimovich,[7] and our group.[8,9] As an idealized special case, all of these studies have given results for thermodynamically symmetric ABC triblocks, with $\chi_{AB} = \chi_{BC}$ and equal statistical segment lengths for all monomer types. The space of SCF solutions for such symmetric systems can be parametrized by a ratio $k \equiv \chi_{AC}/\chi_{AB}$, a dimensionless measure of segregation $\chi_{AC}N$, and the block volume fractions f_A, f_B, and f_C. In the special case of completely symmetric systems, with $f_A = f_C$, SCF solutions depend only upon the three parameters k, $\chi_{AC}N$ and f_B.

Erukhimovich and co-workers[6,7] have constructed a form of weak-segregation theory (WST) analogous to Leibler's theory of diblock copolymers,[12] and used it to study weakly segregated thermodynamically symmetric ABC triblock copolymer melts.[7] Their WST is valid in the vicinity of a critical point at which, they showed, SCFT can yield a continuous order−disorder transition (ODT) for nonfrustrated ABC triblocks. For thermodynamically symmetric systems, with $\chi_{AB} = \chi_{BC}$, the critical point of interest occurs within the isopleth $f_A = f_C$. Erukhimovich and co-workers have focused on systems that obey the Hildebrand or solubility−parameter approximation, in which $\chi_{ij} \propto (\delta_i - \delta_j)^2$, where δ_i is a solubility parameter for monomer i. Within this approximation, a system with $\chi_{AB} = \chi_{BC}$ and $\delta_A \neq \delta_C$ must have $\delta_B = (\delta_A + \delta_C)/2$. The Hildebrand approximation for a symmetric system then necessarily yields $\chi_{AC} = 4\chi_{AB}$, or $k = 4$. This group therefore used WST to calculate a phase diagram for symmetric ABC triblocks with $k = 4$ in the vicinity of this critical point.

Matsen[5] studied ABC triblocks using numerical SCFT, and only considered completely symmetric systems, with $f_A = f_C$. Matsen showed two-dimensional phase diagrams for systems with a fixed value of $k = 1$, over a range of values of f_B and $\chi_{AC}N$, and for systems with a fixed value of $\chi_{AB}N = 50$, over a range of values of f_B and k, with $0 < k < 2$. Matsen thus focused on values of k significantly lower than the value $k = 4$ suggested by the Hildebrand approximation.

Our own theoretical work[8,9] used numerical SCFT to study two models in which the parameters were chosen to approximate those relevant to an extensive series of experiments on poly(isoprene-*b*-styrene-*b*-ethylene oxide) (ISO) triblocks.[13,14] We first considered a somewhat idealized symmetric model with $\chi_{AC}N = 35$ and $\chi_{AB}N = \chi_{BC}N = 13$, or $k = 2.7$, and calculated equilibrium structures for the entire composition triangle at fixed values of $\chi_{ij}N$. We also considered a more realistic slightly asymmetric model in which we used literature values for all statistical segment lengths and interaction parameters.

The structures considered in these previous theoretical studies have included: disordered (D) and lamellar (L) phases, core−shell versions of the gyroid (G), hexagonal cylinder (C), body-centered cubic (BCC) sphere phases (S), "alternating" versions of the gyroid (G^A), diamond (D^A), cylinder (C^A), and sphere (S^A and F^A) phases, and an *Fddd* (or O^{70}) network phase. The alternating phases are structures in which A and C monomers form separate, geometrically similar domains separated by a matrix of B. The G^A phase is a structure with space group $I4_132$, in which A and C domains form interpenetrating networks. The D^A network is a structure with space group $Fd\bar{3}m$, in which A and C domain form interpenetrating diamond networks. Two different alternating sphere structures have been considered, in which A and C spheres are packed on either a CsCl lattice (S^A), which is the alternating version of the BCC phase, or on a NaCl lattice (F^A), in which A and C domains each form a face-centered cubic (FCC) lattice.

*Corresponding author.

 Published on Web 05/17/2010

Previous work suggests that the preferred alternating cylinder phase in moderately to strongly segregated systems is one in which A and C cylinders are packed in a checkerboard pattern, with a square Bravais lattice. To show this, Matsen[5] considered an alternating cylinder phase with rectangular Bravais lattice that can accommodate either a hexagonal or square unit cell, and found that a square unit cell yields the lowest free energy. In a slightly earlier strong-stretching theory of ABC triblocks, Phan and Fredrickson[4] also assumed a square unit cell for the C^A phase. The C^A phase that we consider here is thus based on a square lattice. In his weak-segregation theory, however, Erukhimovich,[7] only allowed for the possibility of a cylinder phase with hexagonal symmetry, because (he showed) the square packing is not expected to be stable in the weak-segregation limit.

In their weak segregation studies of diblock copolymers and ABC triblock copolymers, respectively, Leibler[12] and Erukhimovich[7] both considered a phase that they referred to as an FCC phase. The primary basis function for this phase is constructed from a superposition of the 8 {111} plane waves of a cubic crystal. All coefficients of the plane waves in this structure are real numbers with equal magnitude, but the coefficients of some waves are opposite in sign from others. A weak-segregation representation of a true FCC crystal, which has space group $Fm\bar{3}m$, would instead be constructed as superposition of {111} plane waves with equal, positive real coefficients. Leibler concluded that this phase is never stable in the WST for diblock copolymers, but Erukhimovich concluded that it is stable in symmetric ABC triblock copolymers in a small region near the critical point. With the help of Prof. Erukhimovich (who reviewed this manuscript), we found that the primary basis function of the "FCC" phase discussed by these authors is invariant under the elements of space group $Fd\bar{3}m$ (number 227), which is the space group of the alternating diamond structure considered by Matsen. We also confirmed that this basis function generates a diamond network morphology for each minority component, and so will refer to this hereafter as an alternating diamond (D^A) phase.

Matsen's work on ABC triblocks was motivated in part by experimental work by Mogi and co-workers[15−18] who claimed to have identified an alternating diamond (D^A) phase. Matsen calculated free energies for both D^A and alternating gyroid (G^A) phases, as well as the C^A phase, both types of alternating spheres, and lamellae. He found a substantial region in which G^A phase is stable, but did not find a stable D^A phase within the range of parameters that he considered. Matsen also reexamined the X-ray scattering and electron microscopy data presented by Mogi et al., and argued that this experimental evidence was also more consistent with a G^A structure than with D^A.

Several notable differences emerge from a comparison of the results of previous SCFT studies of completely symmetric systems, with $f_A = f_C$:

Continuous vs Discontinuous ODTs. Erukhimovich predicted a continuous (second order) ODT for completely symmetric systems with $k = 4$ for all values of $\chi_{AC}N$. Similarly, we found a continuous ODT in a numerical SCFT study of systems with $k = 2.7$ at $\chi_{AC}N = 35$. Matsen, however, found only discontinuous (first order) ODTs over the range of parameters that he studied.

Phase Sequence along the ODT. Matsen and Erukhimovich obtained somewhat different results for the sequence of ordered phases encountered along the ODT of completely symmetric systems with increasing f_B. In systems with $k = 1$, Matsen found a phase sequence $L \rightarrow G^A \rightarrow C^A \rightarrow S^A$ as he traced along a line of first order ODTs. In systems with $k = 4$, Erukhimovich found a phase sequence $L \rightarrow G^A \rightarrow D^A \rightarrow S^A$ along a line of continuous ODTs (a critical line).

Phase Sequence away from ODT. Upon moving away from the ODT by decreasing f_B in moderately segregated systems with fixed values of $\chi_{ij}N$, Matsen found a characteristic phase sequence $D \rightarrow S^A \rightarrow C^A \rightarrow G^A \rightarrow L$ in systems with $k = 1$ and $\chi_{AC}N \gtrsim 20$. In symmetric systems with $k = 2.7$ and $\chi_{AC}N = 35$, we reported a corresponding phase sequence $D \rightarrow S^A \rightarrow G^A \rightarrow L$. Notably, we found no stable C^A phase, though we did allow for the possibility. Erukhimovich's WST suggests a phase sequence $D \rightarrow S^A \rightarrow D^A \rightarrow G^A \rightarrow L$ in systems for which $\chi_{AC}N$ is large enough to exhibit an S^A phase near the critical point, though this comparison arguably pushes the WST outside its region of validity.

One goal of the present work is to place the results of these earlier studies for compositionally symmetric systems in a common context, by considering how the predicted phase diagrams for systems with $f_A = f_C$ evolves with changes in the ratio k over the range $k = 1$ to $k = 4$. As part of this, we extend Erukhimovich's results for the value $k = 4$ suggested by the Hildebrand approximation by giving accurate numerical SCFT results, and by allowing for a C^A phase with a square lattice. Our numerical SCF results for such completely symmetric systems are given in section III.

In section IV of this paper, we report results for the composition dependence of the phase behavior for both symmetric and slightly asymmetric models of nonfrustrated ABC triblocks in the intermediate segregation regime. Earlier work by our group[8,9] reported phase diagrams as functions of composition (Gibbs composition triangles) at fixed values of $\chi_{ij}N$ for two models of nonfrustrated triblock copolymers. The parameters used in this work were chosen to match related experiments on ISO triblocks,[13,14] for which the molecular weights were chosen to yield experimentally accessible ODTs. This choice of parameters yielded rather weakly segregated structures in the most interesting parts of the phase diagram. In more recent experiments on higher molecular weight ISO samples, Epps et al.[19] found a network-like structure with no long-range order at compositions for which an *Fddd* phase had been found previously in lower molecular weight samples. Epps et al. proposed that the equilibrium state in these samples might also be a periodic network, possibly *Fddd*, but that long-range order may not form because of the slower kinetics of more strongly segregated systems. In the case of diblock copolymers, however, SCFT theory predicts the *Fddd* phase to be stable only in the weak segregation regime. This raised the question in our minds of whether this particular network morphology might also become less stable relative to competing morphologies with increasing segregation strength in ABC triblock copolymer melts. To examine the molecular weight dependence of the predicted equilibrium phase behavior, we have thus extended our earlier study of ISO triblocks to longer chain lengths. Specifically, we have calculated Gibbs phase triangles at fixed total chain length N for the two models of ISO considered previously, using the same values for the Flory−Huggins interaction parameters and statistical segment lengths, but using values of N that are exactly twice those considered previously.

II. Weak Segregation Theory

The weak segregation theory of Erukhimovich and coworkers[6,7] provides a natural starting point for understanding the phase behavior of symmetric ABC triblock copolymers near the ODT. This work is a relatively straightforward generalization of Leibler's WST of diblock copolymer polymers.[12,20,21] Erukhimovich et al. predicted the existence of a critical point in the phase diagram of approximately symmetric, nonfrustrated ABC triblock copolymers, in which the system can potentially undergo a continuous order−disorder transition. For thermodynamically symmetric triblocks, with $\chi_{AB} = \chi_{BC}$ and equal statistical segment lengths, this critical point must lie within the isopleth

$f_A = f_C$ as a result of a symmetry under interchange of the A and C blocks. The symmetry argument requiring the existence of a line of critical points within this isopleth is very similar to the argument requiring the existence of a critical point along with line $f_A = f_B$ in diblock copolymers with equal statistical segment lengths. Here, we recapitulate a few results of the WST that are potentially useful as a guide to numerical SCFT studies.

The weak segregation theory for any block copolymer melt is based on a Taylor expansion of the free energy about that of a homogeneous phase. Let $\psi_i(\mathbf{r})$ denote the ensemble average

$$\psi_i(\mathbf{r}) = \langle \delta c_i(\mathbf{r}) \rangle \tag{1}$$

of the deviation $\delta c_i(\mathbf{r})$ of the concentration of monomers of type i at position $\mathbf{r}$ from its value in the homogeneous state. Let $F[\psi]$ denote the free energy functional of an ABC triblock copolymer melt, expressed as a functional of the three fields $\psi \equiv \{\psi_A(\mathbf{r}), \psi_B(\mathbf{r}), \psi_C(\mathbf{r})\}$. We consider an expansion of the deviation $\delta F[\psi]$ of this free energy from its value in the homogeneous state, of the form

$$\delta F \simeq \frac{1}{2}\int \frac{d\mathbf{q}}{(2\pi)^3}\Gamma^{(2)}_{ij}(\mathbf{q})\psi_i(\mathbf{q})\psi_j(-\mathbf{q}) + \frac{1}{3!}\int \frac{d\mathbf{q}_1 d\mathbf{q}_2}{(2\pi)^6}\Gamma^{(3)}_{ijk}(\mathbf{q}_1,\mathbf{q}_2,\mathbf{q}_3)\psi_i(\mathbf{q}_1)\psi_j(\mathbf{q}_2)\psi_k(\mathbf{q}_3) + \ldots \tag{2}$$

where $\psi_i(\mathbf{q}) \equiv \int d\mathbf{r}\, e^{i\mathbf{q}\cdot\mathbf{r}}\psi_i(\mathbf{r})$, and where $\mathbf{q}_3 \equiv -\mathbf{q}_1 - \mathbf{q}_2$ in the second line.

In what follows, we consider a melt in which each monomer occupies a volume $v_0 = 1/c$, where c is the overall monomer concentration. We focus on the incompressible limit, in which we require that

$$\sum_i \psi_i(\mathbf{q}) = 0 \tag{3}$$

for all $\mathbf{q}$.

A. Limit of Stability. To identify the limit of stability of the homogeneous state, it is sufficient to consider the second order coefficient $\Gamma^{(2)}_{ij}(\mathbf{q})$ in the above expansion. This quantity is equal to the matrix inverse $\Gamma^{(2)}_{ij}(\mathbf{q}) = S_{ij}^{-1}(\mathbf{q})$ of the correlation function

$$S_{ij}(\mathbf{q}) = \int d\mathbf{r}\, \langle \delta c_i(\mathbf{r})\delta c_i(0)\rangle e^{i\mathbf{q}\cdot\mathbf{r}} \tag{4}$$

The random-phase approximation (RPA) for $\Gamma^{(2)}_{ij}(\mathbf{q})$ for an ABC block terpolymer may be expressed compactly as a sum

$$\Gamma^{(2)}_{ij}(\mathbf{q}) = \Omega_{ij}^{-1}(\mathbf{q}) + V_{ij} \tag{5}$$

Here, V_{ij} is an effective interaction that is assumed to be approximately independent of q, and $\Omega_{ij}^{-1}(\mathbf{q})$ is the matrix inverse of an intramolecular correlation function $\Omega_{ij}(\mathbf{q})$. More precisely, $\Omega_{ij}(\mathbf{q})$ is the intramolecular contribution to $S_{ij}(\mathbf{q})$, which arises from correlations between pairs of monomers of types i and j belonging to the same chain. The effective interaction V_{ij} in a slightly compressible liquid may be expressed as a sum

$$V_{ij} = v_0(B + \chi_{ij}) \tag{6}$$

where B is a nondimensional compression modulus, and χ_{ij} is a matrix of Flory−Huggins interaction parameters.

The incompressible limit may be recovered from the above formulation by taking $B \to \infty$. As a matter of convention, we take the diagonal elements of χ_{ij} to vanish ($\chi_{ii} = 0$) when discussing this limit. As $B \to \infty$, one of the eigenvectors of the 3×3 matrix $\Gamma^{(2)}_{ij}(\mathbf{q})$ approaches a pure "compression" mode of the form $\varepsilon = (1,1,1)$, for which the corresponding eigenvalue increases linearly with B. The other two eigenvectors of $\Gamma^{(2)}_{ij}(\mathbf{q})$ are "composition" modes whose eigenvalues approach finite limits as $B \to \infty$. Fluctuations of the compression mode, which is a variation of overall monomer density at fixed composition, are strongly suppressed. The two composition fluctuation modes must be orthogonal to ε, because the eigenvectors of a real symmetric matrix must be orthogonal. This mathematical statement is equivalent to the physical requirement that, in the limit $B \to \infty$, the two composition modes of interest lie within the subspace of vectors that satisfy constraint 3.

The projection of $\psi_i(\mathbf{q})$ onto a two-dimensional subspace of composition fluctuations may be made more explicit by introducing two appropriate basis vectors. Let $e^{(1)}$ and $e^{(2)}$ represent two orthonormal basis vectors that satisfy constraint 3, so that $\varepsilon \cdot e^{(1)} = \varepsilon \cdot e^{(2)} = 0$ and $e^{(\alpha)}e^{(\beta)} = \delta_{\alpha\beta}$ for α, $\beta = 1, 2$. We may expand any composition fluctuation $\psi_i(\mathbf{q})$ that satisfies the constraint in terms of these basis vectors, as a sum

$$\psi_i(\mathbf{q}) = \varphi_1(\mathbf{q})e_i^{(1)} + \varphi_2(\mathbf{q})e_i^{(2)} \tag{7}$$

The quadratic approximation for the free energy for pure composition fluctuations may then be expressed as a sum

$$\delta F[\phi] \simeq \frac{1}{2}\int \frac{d\mathbf{q}}{(2\pi)^3}\gamma_{\alpha\beta}(\mathbf{q})\varphi_\alpha(\mathbf{q})\phi_\beta(-\mathbf{q}) \tag{8}$$

in which

$$\gamma_{\alpha\beta}(\mathbf{q}) = \sum_{i,j}\Gamma^{(2)}_{ij}(\mathbf{q})e_i^{(\alpha)}e_j^{(\beta)} \tag{9}$$

is a reduced 2×2 matrix whose elements are independent of B in the limit $B \to \infty$.

The homogeneous phase of an incompressible liquid is locally stable when both eigenvalues of the matrix $\gamma^{(2)}(\mathbf{q})$ are positive for all $\mathbf{q}$. Let $\lambda_1(\mathbf{q})$ and $\lambda_2(\mathbf{q})$ represent the two eigenvalues of $\gamma^{(2)}(\mathbf{q})$ at a specified wavevector $\mathbf{q}$ and a specified set of values of $\chi_{ij}N$. These are equal to the two eigenvalues of the 3×3 matrix $\Gamma^{(2)}_{ij}(\mathbf{q})$ that are associated with the composition modes. Let $\mathbf{q}_i^*$ be the wavevector at which eigenvalue $\lambda_i(\mathbf{q})$ is minimum. The spinodal surface is the surface in the space of values of $\chi_{ij}N$ and volume fractions f_A, f_B and f_C along which $\lambda_i(\mathbf{q}_i^*) = 0$ for one of the two eigenmodes (the "critical" mode) while the other eigenvalue generally remains positive. The limit of stability in an incompressible ABC block copolymer melt is thus controlled by a competition between two potential instabilities that generally involve spatial modulations with different critical wavenumbers q_1^* and q_2^*. The spinodal surface can also contain a subsurface of "double critical points" within which both eigenvalues vanish, across which the identity of the critical mode changes discontinuously.[6,7,22]

Consider a family of systems constructed from a specified set of monomers, with fixed values of χ_{ij} and fixed statistical segment lengths. The parameter space for this family of systems can be visualized as a triangular prism, in which the vertical direction represents N, and a horizontal triangle obtained at fixed N represents a Gibbs composition triangle. Each of the three vertical faces contains a diblock copolymer phase diagrams as a function of one composition and N. The spinodal surface is a 2D surface within this prism.

B. Critical Points. A critical point is a point within the spinodal surface at which a continuous (i.e., second-order) ODT is possible. Mathematically, this can occur only at points within the spinodal surface at which there is a vanishing value of the third (as well as second) derivative of the free energy which respect to the amplitude of the critical mode. For each point on the spinodal surface, we may identify a critical eigenvector $v = v(q^*)$ of $\Gamma^{(2)}_{ij}(\mathbf{q}^*)$ for which the corresponding eigenvalue vanishes. A critical point is a point within the spinodal surface at which

$$\Gamma^{(3)}_{ijk}(\mathbf{q}_1, \mathbf{q}_2, \mathbf{q}_3) v_i v_j v_k = 0 \tag{10}$$

for any set of wavevectors of magnitude $|\mathbf{q}_1| = |\mathbf{q}_2| = |\mathbf{q}_3| = q^*$ for which $\mathbf{q}_1 + \mathbf{q}_2 + \mathbf{q}_3 = 0$. In the WST for either diblocks or triblocks, values of $\Gamma^{(n)}$ for $n \geq 3$ are independent of the interaction parameters, and depend on N only through an overall prefactor of $c^{n-1}N^{-1}$. The matrix $\Gamma^{(3)}_{ij}(\mathbf{q}_i, \mathbf{q}_j, \mathbf{q}_k)$ in eq 10 may thus be expressed as a function of composition alone, times a prefactor of $1/c^2N$. The solutions to eq 10 do, however, generally depend upon the interaction parameters because the critical eigenvector v generally depends upon the interaction parameters.

For a family of systems with fixed values of χ_{ij} and b_i, where b_i are statistical segment lengths, eq 10 can generally be satisfied only along one or more lines within the two-dimensional spinodal surface. Each of the three pure diblock copolymer systems for ij diblocks contains one critical point, which occurs at $f_i = f_j = 0.5$ and $\chi_{ij}N = 10.495$ for systems with $b_i = b_j$. In the systems of interest here, the solutions of eq 10 define at least two lines of critical points within the spinodal surface, which terminate at the three critical points of the three diblock copolymer systems and at the corner $f_B = 1$ of pure B homopolymer.

C. Symmetric Triblocks. The above analysis applies to arbitrary triblock copolymers. We now consider the case of completely symmetric triblocks with $b_A = b_B = b_C$, $\chi_{AB} = \chi_{BC}$, and $f_A = f_C$, and consider the effect of varying $k \equiv \chi_{AC}/\chi_{AB}$. For such systems, $\Gamma^{(2)}_{ij}(\mathbf{q})$ is invariant under relabeling of A and C ends of the chain. As a result of this symmetry, the eigenvectors of $\Gamma_{ij}(\mathbf{q})$ must all be either even or odd under this change of labels. This symmetry, combined with incompressibility, enables us to identify the normalized eigenmodes as

$$v^{(AC)} = (1, 0, -1)/\sqrt{2}$$

$$v^{(B)} = (1, -2, 1)/\sqrt{6} \tag{11}$$

Note that $v^{(AC)}$ is the only normalized vector that is odd under exchange of A and C, while $v^{(B)}$ is the only vector that is orthogonal to both $v^{(1)}$ and the compression mode (1,1,1). We refer to $v^{(AC)}$ as an AC modulation (as indicated by the superscript "AC") because it represents a deviation that tends to segregate A and C into different domains. We refer to $v^{(B)}$ as a B modulation because it leads to segregation of B regions from regions containing an equal mixture of A and C monomers.

The AC mode satisfies critical condition 10 whenever $f_A = f_C$, independent of f_B. This is a result of the symmetry between A and C monomers,[7] since $v_i^{(AC)} v_j^{(AC)} v_k^{(AC)}$ is antisymmetric with respect to the relabeling of A and C block but $\Gamma^{(3)}_{ijk}$ is symmetric. The line where the spinodal surface crosses the plane $f_A = f_C$ is thus a line of critical points. Numerically calculating $\Gamma^{(3)}_{ijk}$ shows that the $e^{(B)}$ mode satisfies eq 10 within the plane $f_A = f_C$ only when $f_B = 0.49$.

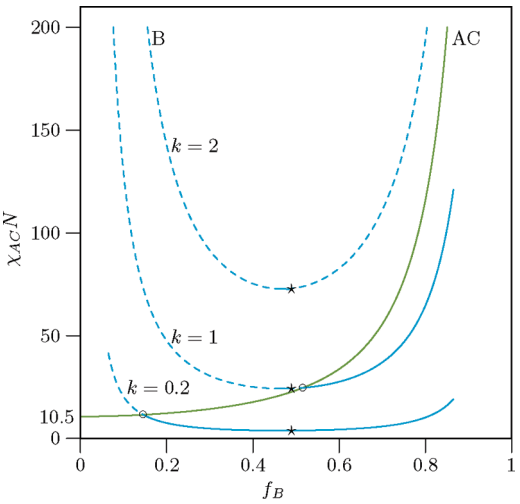

Figure 1. Spinodals of symmetric ABC triblock copolymers within the AC isopleth, $f_A = f_C$. The AC modulated spinodal, labeled AC, is independent of k. B modulated spinodals are shown for three values of k ($k = 0.2$, 1, and 2). Portions of the B modulated spinodals that are preempted by the AC spinodal are shown dashed. The double spinodal points at which the AC and B spinodals intersect for $k < 2$ are marked by open circles. The critical point at $f_B = 0.49$ on each B modulated spinodal is marked by a star.

The two corresponding eigenvalues of $\Gamma^{(2)}_{ij}(\mathbf{q})$, denoted $\lambda_{AC}(\mathbf{q})$ and $\lambda_B(\mathbf{q})$, may be calculated by contracting $\Gamma^{(2)}_{ij}(\mathbf{q})$ with the above eigenvectors. This yields

$$cN\lambda_{AC}(\mathbf{q}) = F_{AC}(\mathbf{q}) - \chi_{AC}N \tag{12}$$

$$cN\lambda_B(\mathbf{q}) = F_B(\mathbf{q}) + (\chi_{AC}N - 4\chi_{AB}N)/3 \tag{13}$$

where c is overall monomer concentration, and

$$F_\alpha(\mathbf{q}) \equiv cN\Omega^{-1}_{ij}(\mathbf{q}) v_i^{(\alpha)} v_j^{(\alpha)} \tag{14}$$

for α = AC or α = B. The limit of stability of the homogeneous phase with respect to the AC modulation, at which $\lambda_{AC}(\mathbf{q}^*_{AC}) = 0$, occurs when

$$\chi_{AC}N = F_{AC}(\mathbf{q}^*_{AC}) \tag{15}$$

The corresponding limit of stability for the B mode in a system with a fixed value of $k = \chi_{AC}/\chi_{AB}$, occurs when

$$\chi_{AC}N = \frac{3k}{4-k} F_B(\mathbf{q}^*_B) \tag{16}$$

The quantities $F_{AC}(\mathbf{q}^*_{AC})$ and $F_B(\mathbf{q}^*_B)$ are functions of f_B alone. These functions are positive for all f_B, as required to guarantee the stability of the homogeneous phase in the limit $\chi_{AC} = \chi_{BC} = 0$. In the limit $f_B \to 0$, the AC instability becomes the instability of a symmetric AC diblock copolymer, and so eq 15 yields a critical value $\chi_{AC}N = 10.495$ when $f_B = 0$. Note that the value of $\chi_{AC}N$ along the AC stability line is completely independent of $\chi_{AB}N$. Also note that a B modulated instability with $\chi_{AC} > 0$ can exist only for $0 < k < 4$, since eq 16 has a positive solution only in this range of values.

In Figure 1, we have plotted the AC-modulated spinodal of eq 15, which is independent of k, and the B-modulated spinodal for $k = 0.2$, $k = 1$, and $k = 2$. The value of $\chi_{AC}N$ along the AC-modulated spinodal approaches 10.495 as $f_B \to 0$, increases monotonically with increasing f_B, and diverges as $f_B \to 1$.

The value of $\chi_{AC}N$ along the B modulated spinodal diverges at both $f_B = 0$ and $f_B = 1$, and has a minimum at the fixed composition $f_B = 0.47$, where the function $F_B(\mathbf{q}_B^*, f_B)$ is minimum. The value of $\chi_{AC}N$ along the B-modulated spinodal also increases monotonically with k in the range $0 < k < 4$, due to the prefactor of $k/(4 - k)$ in eq 16, and diverges for all f_B as $k \rightarrow 4$.

For values of $k > 4$, only the AC-modulated spinodal exists. For $2 < k < 4$, both AC and B spinodals exist, but the AC spinodal always preempts the B spinodal. For $k < 2$, the two spinodals intersect at a "double spinodal point"[22] at some composition $f_B = f_{DSP}$ that decreases with decreasing k. For $k < 2$, the nature of the true spinodal is AC modulated for $f_B < f_{DSP}$ and B modulated for $f_B > f_{DSP}$.

D. Weakly-Segregated Ordered Phases. Near the critical point of an ABC copolymer, the structure of most of the ordered phases may be approximated by a single-wavenumber approximation in which we take

$$\psi_i(\mathbf{r}) \simeq A v_i f(\mathbf{r}) \tag{17}$$

where A is an order parameter amplitude, v is the critical mode of $\Gamma_{ij}^{(2)}(\mathbf{q}^*)$, and $f(\mathbf{r})$ is a primary basis function of the form

$$f(\mathbf{r}) = \frac{1}{\sqrt{2m}} \sum_{i=1}^{m} (e^{i\mathbf{q}_i \cdot \mathbf{r} + \phi_i} + c.c.) \tag{18}$$

Here, the $2m$ wavevectors $\pm \mathbf{q}_1, ..., \pm \mathbf{q}_m$ are all wavevectors of equal magnitude $|\mathbf{q}_i| = q^*$ that comprise the primary shell of the reciprocal lattice for a candidate crystal structure. The assumption in eq 18 that the coefficients of all $2m$ plane waves have the same amplitude, though possibly different phases, is correct if these plane waves are all related to one another by elements of the relevant space group. The only known candidate structure in which the wavevectors of the primary shell are not all related by symmetry is the *Fddd* phase,[23] which we will thus not discuss further. If the function $f(\mathbf{r})$ is invariant under a space group that contains no glide plane or screw axis symmetries, the phases $\phi_1, ..., \phi_m$ must all be equal. If the space group does contain glide planes or screw axes, these symmetries generally impose nontrivial relationships among these phases.

All of the 3-dimensional phases that we consider here are cubic, except the *Fddd* phase. Most of these phases have been well described elsewhere, so we limit ourselves here to a few clarifying comments. The primary basis function $f(\mathbf{r})$ for the diblock copolymer BCC phase (space group $Im\bar{3}m$) is a superposition of the 12 wavevectors in the {110} family, with equal phases. The structure that we call an "alternating" BCC (S^A) phase (space group $Pm\bar{3}m$) is instead based on a simple cubic crystal, since the A-rich and C-rich domains each form a simple cubic lattice. The primary basis function for the S^A phase is thus constructed from the 6 {100} wavevectors. The FCC phase of a diblock copolymer and the alternating F^A phase are both structures with space group $Fm\bar{3}m$, in which the A and (in a triblock copolymer melt) C domains are each organized on an FCC lattice. The FCC phase of an AB diblock copolymer can thus be continuously evolved into the NaCl structure of the F^A phase of a symmetric ABC triblock by "growing" an FCC lattice of C domains in the interstices of the lattice of A domains. The primary basis function for this phase is a superposition of {111} wavevectors with equal real coefficients. The phase that both Leibler[12] and Erukhimovich[7] referred to as an FCC phase, however, is a superposition of {111} wavevectors with real coefficients of both signs. If we define $\mathbf{q}_1 \equiv (\bar{1}11)2\pi/a$, $\mathbf{q}_2 \equiv (1\bar{1}1)2\pi/a$, $\mathbf{q}_3 \equiv (11\bar{1})2\pi/a$, and $\mathbf{q}_4 \equiv (111)2\pi/a$, then phase relationship given in eq V-30 of ref 12 and in eq 20 of ref 7 can be satisfied by choosing phases $\phi_1 = \phi_2 = \phi_3 = 0$ but $\phi_4 = \pi$. The resulting basis function can be shown to be invariant under the elements of space group of $Fd\bar{3}m$. This function is also equivalent to the one used by Thomas and co-workers,[24] given in their eq 13, to generate a level set surface with the diamond topology of Schwarz's D minimal surface. This structure is thus most accurately described as a diamond or (for ABC triblocks) an alternating diamond phase.

III. SCFT for Symmetric Systems ($f_A = f_C$)

In this section, we use numerical SCFT to examine how the phase diagrams of symmetric ABC triblocks within the AC-isopleth change due to changes in the ratio $k = \chi_{AC}/\chi_{AB}$. In order to bridge the results of Matsen ($k = 1$) and Erukhimovich ($k = 4$) we have prepared phase diagrams at $k = 1$, $k = 2$, and $k = 4$.

The algorithms used in our SCFT calculations have been described previously.[25,26] We solve the modified diffusion equation using a variant of the pseudospectral integration algorithm,[27] in which we use Richardson extrapolation to obtain an algorithm that is accurate to fourth order in the contour length step size Δs.[26] An Adams−Bashford integration algorithm with the same order of accuracy has been presented by Cochran, Fredrickson et al.[28] To study phases with specific space group symmetries, we use a representation of the chemical potential field in terms of symmetry adapted basis functions similar to those introduced by Matsen and Schick, to create initial conditions and to iterate the SCF equations. An algorithm for automatically generating basis functions for any space group is described in an appendix of ref 29 and in ref 30. The free energy is optimized with respect to variations in unit cell dimensions by adding a condition of zero stress to the list of residuals in a quasi-Newton iteration scheme.[25] Iteration of the self-consistency and stress equations is carried out using a Newton−Broyden scheme in which an initial approximation for the Jacobian is obtained by using finite differences to calculate the response to changes in unit cell dimensions and long-wavelength components of the chemical potential fields, but in which the response to short wavelength components is approximated by using a random-phase approximation for the linear response of a homogeneous melt. A Broyden scheme is used to update this initial Jacobian. The Fortran 90 program, named PSCF, that we use for such calculations is available via links from the Morse research group web page.

In the work presented here, we calculate phase diagrams for symmetric systems with $k = 1$, 2, and 4 by comparing free energies for the disordered (D) and the ordered S^A, F^A, C^A, D^A, G^A and L phases. All of these ordered phases are alternating, or AC-modulated, structures. The stability analysis given in section II also suggests the possibility of finding B modulated phases at values of $k < 2$ and large enough values of f_B or $\chi_{AC}N$. A B-modulated phase is one that contains B-rich domains and domains in which A and C remain mixed in equal proportions, so that the ordered structure is invariant under interchange of the identities of A and C monomers.

At the lowest value of k that we consider, $k = 1$, the spinodal is AC modulated only for $f_B < 0.51$ and is B-modulated for $f_B > 0.51$. By itself, this analysis suggests that one might need to allow for B modulated phases at $k = 1$ and large values of f_B. Matsen has already studied this part of the phase diagram, however, while allowing for B-modulated phases (which he denoted by symbols with primes, such as L′, C_h'), and did not find them to be stable in any systems with $k = 1$. Matsen did find B modulated phases in a systems with $\chi_{AB}N = 50$ and variable k, but only at somewhat lower values of k. On the basis of this earlier work, we thus do not expect to find B-modulated phases over the range $k = 1-4$ considered here.

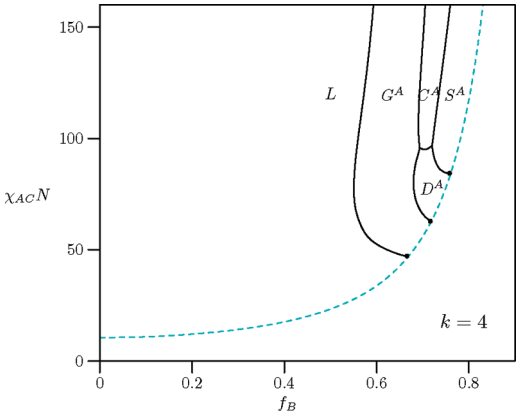

Figure 2. Phase diagram of symmetric ABC triblock copolymers within the AC isopleth, for $k = \chi_{AC}/\chi_{AB} = 4$. The dashed line is the spinodal for the AC modulated instability, and also a line of second-order ODTs. The ODT is second-order throughout the range of parameters considered here.

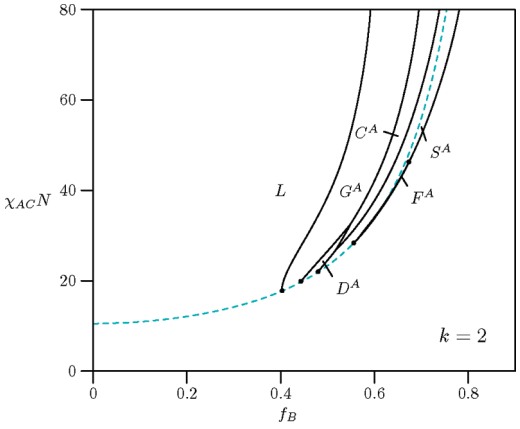

Figure 3. Phase diagram of symmetric ABC triblock copolymers within the AC isopleth, for $k = \chi_{AC}/\chi_{AB} = 2$. The dashed line is the spinodal for the AC modulated instability, which coincides with the ODT for small values of f_B. The F^A phase is found to be stable over a very narrow region near the ODT, which is too narrow to see in this figure, within the region between the dots along the ODT line.

Our results for $k = 4$, $k = 2$, and $k = 1$ are presented in Figures 2, 3, and 4, respectively. Discontinuous order−order transitions (OOTs) and ODTs are shown by solid lines, while AC- and B-modulated spinodal lines and continuous ODTs are shown by dashed lines. Where continuous transitions occur, they always correspond to the AC-modulated instabilities, and coincide with the AC-modulated spinodal line. For all values of k, the ODT becomes a continuous AC modulated transition to a lamellar phase in the limit $f_B \to 0$, where a line of AC modulated critical points merges with the critical point of an AC diblock copolymer.

Our results for $k = 4$ are shown in Figure 2. For this value of k, we find a continuous ODT exactly along the spinodal line up to the highest value of $\chi_{AC}N = 80$ that we considered, as predicted by Erukhimovich's WST. The sequence of ordered phases encountered along the ODT with increasing f_B is L → G^A → D^A → S^A. Along the ODT we find L for $f_B < 0.665$, G^A for $0.665 < f_B < 0.716$ and D^A for $0.716 < f_B < 0.758$. These results for behavior near the ODT are completely consistent with the WST results of Erukhimovich, including his prediction of a region of stable alternating diamond phase (which he referred to as an FCC phase), and the range of compositions over which each phase is encountered. Further from the ODT line, however, we find the appearance of an square alternating cylinder (C^A) phase and the disappearance of the D^A phase. Upon moving away from the

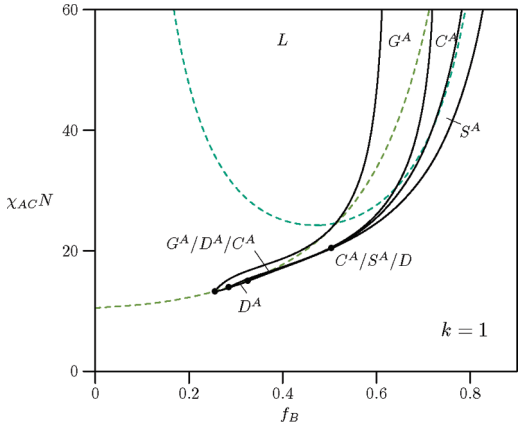

Figure 4. Phase diagram of symmetric ABC triblock copolymers within the AC isopleth, for $k = \chi_{AC}/\chi_{AB} = 1$. The dashed lines are the spinodals for the AC modulated and B modulated instabilities. The ODTs are first order for the transitions from the disordered (D) phase to the G^A, C^A, and S^A phases, but second order (continuous) for the transition to the lamellar (L) phase.

ODT by decreasing f_B at relatively large, fixed values of $\chi_{AC}N$, we find the phase sequence D → S^A → C^A → G^A → L found by Matsen. Our results are consistent with the observation that the square C^A is disfavored by the rules of WST very near the ODT, and indicate that the C^A phase is preferred over D^A in more strongly segregated symmetric triblocks.

Figure 3 shows the phase diagram for systems with $k = 2$. The topology of the phase diagram is similar to that obtained for $k = 4$, except that the overall scale of $\chi_{AC}N$ decreases, and that the ODT becomes first order for large values of f_B and $\chi_{AC}N$. There is still a region in which the D^A phase is stable near the ODT, but it is considerably smaller than for $k = 4$. This phase diagram also contains an extremely narrow sliver (not visible at this scale) in which an F^A phase is stable near the first order ODT, in the region between the two dots on the ODT line. The ODT becomes discontinuous for compositions with $f_B \gtrsim 0.6$, but seems to still be continuous for the L−D and G^A−D transitions, for which the ODT coincides with the AC spinodal.

Figure 4 shows the phase diagram for the case $k = 1$ considered previously by Matsen. Our results agree with those of Matsen, who only gave results for $f_B > 0.4$, and extend his results to lower values of f_B, where the ODT becomes continuous. We show both the AC- and B-modulated spinodal lines for comparison. In this case, we find that the C^A phase remains stable over a very narrow region near the first-order ODT, until it ends at even smaller region in which the D^A phase is stable very near the ODT. The sliver in which the C^A phase is stable near the ODT is difficult to see on this scale, but was also found in Matsen's work. In this case, we find no F^A phase near the ODT. The region in which the D^A phase is stable near the ODT lies outside the region $f_B > 0.4$ studied by Matsen. The sequence of ordered phase phases along the ODT is thus L → G^A → D^A → C^A → S^A. Other than the L−D transition, all ODTs appear to be discontinuous, consistent with Matsen's conclusions for systems with $f_B > 0.4$.

Matsen[5] has noted previously that the values of f_B along OOTs between ordered phases become almost independent of $\chi_{AC}N$ sufficiently far from the ODT, and depend only on $\chi_{AB}N = \chi_{BC}N$. This is because the A and C domains become well separated from each other in well segregated AC modulated phases, so that the free energies of these phases become independent of χ_{AC}. Our own results are also consistent with this observation.

Upon comparing these results to the stability analysis of section II, we find that the stability analysis provides a reliable guide to the nature of the ordered phases along the ODT, and the order of the transition, only at the highest value of k considered

here, $k = 4$. The simplest assumption, in the absence of numerical SCFT results, would be that the ODT is a continuous transition to an AC modulated phase where the limit of stability of the disordered phase is given by a line of AC modulated critical points, and that the ODT is a discontinuous transition to a B modulated phase where the spinodal is B modulated. At $k = 1$, we instead find a large region of parameter space in which the spinodal is B modulated, but the ODT is a discontinuous transition to an AC modulated structure. At $k = 2$, we find large regions in which a discontinuous transition to an AC modulated structure preempts a potentially continuous transition to an AC modulated structure. Neither of these possibilities is easily allowed for in the weak segregation theory. The WST has, however, provided reliable information about the nature of the ordered phases near the ODT wherever the ODT actually is continuous, and has provided some very useful guidance regarding which phases should be considered as candidates.

IV. Phase Triangles at Intermediate Segregation

In our previous work,[8,9] we considered the composition dependence of the phase diagram for two models with fixed values of $\chi_{ij}N$. One was a symmetric ABC triblock model $\chi_{AC}N = 35$ and $\chi_{AB}N = 13$. The other was a slightly asymmetric model for which values of the both the statistical segment lengths ($b_I = 6.0$ Å, $b_S = 5.5$ Å, $b_O = 7.8$ Å) and the interaction parameters ($\chi_{IS} = 0.044$, $\chi_{SO} = 0.0496$, $\chi_{IO} = 0.1832$, $N = 250$) were taken from the literature, yielding $\chi_{IS}N = 11.0$, $\chi_{SO} = 14.2$, $\chi_{IO} = 45.8$ for $N = 250$. Each of the resulting phase triangles corresponds to a horizontal cut of the phase prism for systems with fixed values of the χ_{ij}'s at a fixed value of N (e.g., $N = 250$ in the asymmetric model). Here, as examples of more strongly segregated nonfrustrated systems, we present phase triangles for the same two models for values of N that are exactly twice those used previously.

Figures 5 and 6 show our results for the symmetric and asymmetric model, respectively. In each figure, part a shows results obtained for the chain length N studied previously, and part b shows new results for chains of length $2N$. Expanded views of the regions near the critical points of the lower molecular weight symmetric and asymmetric systems are shown in Figure 7. Several features are common to both the symmetric and asymmetric models. For both models, we find a sequence of core−shell morphologies near the A and C corners, and a sequence of alternating morphologies near the line $f_A = f_C$. For both models, the phase diagrams for the two different chain lengths are quite similar. The most obvious changes with increasing N are shrinkage of the disordered regions, migration of most order−order transitions toward the corners of the phase diagram, and an increase in the size of the central lamellar region.

We now consider the symmetric model of Figure 5 in more detail. The behavior along the isopleth $f_A = f_C$ of these systems, for which $k = 2.7$ for $\chi_{AC}N = 35$ and 70, may be directly compared to the results shown in section III for $k = 2$ and $k = 4$. We see in Figure 5 that for $k = 2.7$ the phase sequence along this isopleth is $D \rightarrow S^A \rightarrow D^A \rightarrow G^A \rightarrow L$ for $\chi_{AC}N = 35$, with no C^A phase, but the sequence is $D \rightarrow S^A \rightarrow C^A \rightarrow G^A \rightarrow L$ for $\chi_{AC}N = 70$, with a C^A phase but no D^A phase. Both phase sequences, and the replacement of the weakly segregated D^A phase by a C^A phase with increasing segregation, are consistent with the behavior shown in Figures 2 and 3. We find a continuous $D \rightarrow S^A$ ODT along the isopleth for $k = 2.7$ at both $\chi_{AC}N = 35$ and $\chi_{AC}N = 70$. Figure 3 shows, however, that the ODT at $k = 2$ is first order for all $\chi_{AC}N > 30$. This suggests that the point $k = 2.7$ and $\chi_{AC}N = 70$ must be near the boundary between first and second order ODTs. In Figure 5, two thin edges of FCC packed spheres appear along the order−disorder transition in the B-rich corner of part b, but not in part a.

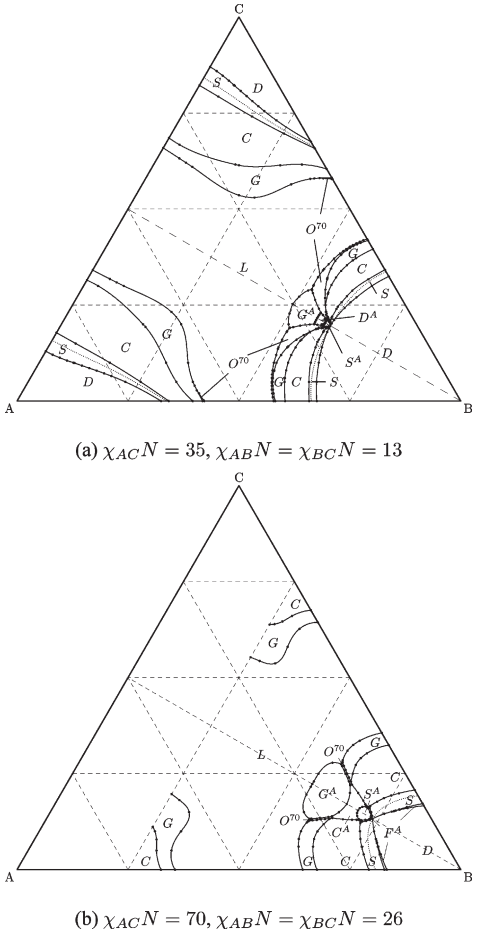

(a) $\chi_{AC}N = 35$, $\chi_{AB}N = \chi_{BC}N = 13$

(b) $\chi_{AC}N = 70$, $\chi_{AB}N = \chi_{BC}N = 26$

Figure 5. Phase diagram in the composition triangle of symmetric an ABC triblock copolymer with $b_A = b_B = b_C$ and for (a) $\chi_{AC}N = 35$ and $\chi_{AB}N = \chi_{BC}N = 13$ and (b) $\chi_{AC}N = 70$ and $\chi_{AB}N = \chi_{BC}N = 26$ for $f_B > 0.25$. Dots along the phase boundaries are the points at which phase boundaries have been accurately determined. The indicated phase boundary lines are simply interpolations between these points. The dotted lines near the ODT in each corner of part a and in the B-rich corner of part b are spinodal lines. A critical point exists in both parts along the symmetry line $f_A = f_C$, where this line intersects the ODT and the spinodal. The ordered phase at this critical point is an alternating BCC (S^A) sphere phase for part a and is alternating FCC (F^A, or NaCl) packing of spheres for part b, though the F^A phase is stable only within a very narrow sliver along the ODT.

One notable difference between parts a and b in Figure 5 for the symmetric model is the shrinkage in part b of the small regions in which the O^{70} phase is stable in part a: In part a ($\chi_{AB}N = 13$), the O^{70} phase is stable throughout a long narrow sliver that reaches the AB and BC diblock edges, while in part b ($\chi_{AB}N = 26$), the O^{70} phase remains stable only within a much smaller region that does not extend to the diblock edges. These results are reminiscent of the results found for symmetric AB diblocks, in which a stable O^{70} phase exists only for $\chi_{AB}N < 13.76$. It seems likely that the remaining O^{70} region disappears at somewhat higher values of $\chi_{AC}N$, but further calculations would be required to show this. In this symmetric model, however, the O^{70} network clearly becomes less stable with increasing N.

Now consider the results shown in Figure 6 for a slightly asymmetric model. Here, we also find both D^A and G^A networks near the critical point in the lower molecular weight system (part a), but a C^A phase and no D^A phase in the higher molecular weight analogue. The most striking difference between our results for symmetric and asymmetric models is the presence in Figure 6, for both chain lengths, of a band of G and O^{70} network phases that connects the OS and IS edges. This band includes a large O^{70}

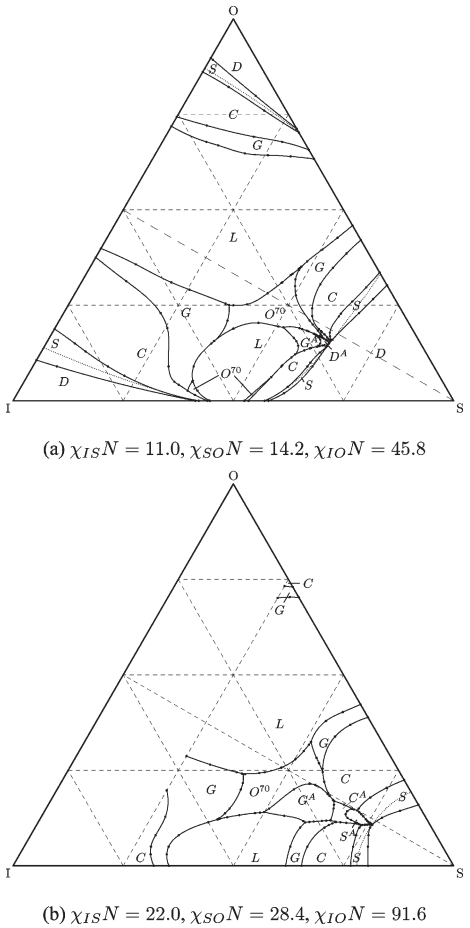

(a) $\chi_{IS}N = 11.0$, $\chi_{SO}N = 14.2$, $\chi_{IO}N = 45.8$

(b) $\chi_{IS}N = 22.0$, $\chi_{SO}N = 28.4$, $\chi_{IO}N = 91.6$

Figure 6. Phase diagram in the composition triangle for poly(isoprene-styrene-ethylene oxide), with statistical segment lengths $b_I = 6.0$ Å, $b_S = 5.5$ Å, $b_O = 7.8$ Å, and interaction parameters: (a) $\chi_{IO}N = 45.8$, $\chi_{IS}N = 11.0$ and $\chi_{SO}N = 14.2$; (b) $\chi_{IO}N = 91.6$, $\chi_{IS}N = 22.0$, and $\chi_{SO}N = 28.4$, shown only for $f_S > 0.25$. Symbols have the same meaning as in Figure 5. The ordered phase at the critical point is G^A for part a and S^A for part b.

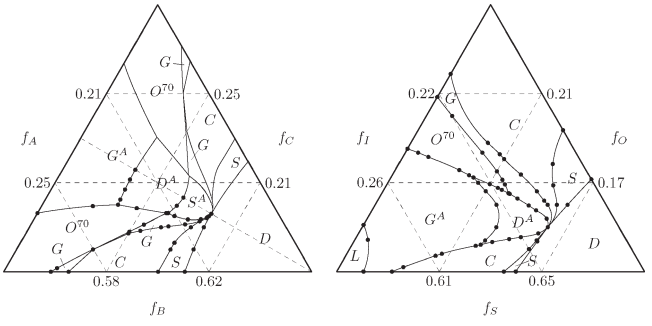

(a) ABC critical region (b) ISO critical region

Figure 7. Expanded views of regions near the critical points of (a) symmetric ABC triblocks with $\chi_{AC}N = 35$, from Figure 5a, and (b) ISO triblocks with $\chi_{IO}N = 45.8$, from Figure 6a.

region where the symmetric model yields a lamellar phase. Unlike the symmetric case, the region in which the O^{70} phase is stable does not shrink with increasing N. In fact, the O^{70} region is slightly enlarged at the higher molecular weight, and spans a range of values of f_C that is actually closer to that which was originally observed experimentally on the lower molecular weight ISO samples. This prediction is consistent with the tentative identification of the "disordered" network found by Epps et al. in higher molecular weight samples[19] as a disordered O^{70} phase. More generally, it indicates that the O^{70} is not confined to the weak segregation regime in modestly asymmetric ABC triblocks, but that the stability of this structure depends very sensitively on the difference between χ_{AB} and χ_{BC}.

The two phase triangles shown above for the lower molecular weight systems (the upper panels of Figures 5 and 6) differ slightly from those we presented previously for the same parameters, as the result of our identification of a stable alternating diamond phase near the critical point. We erred in our earlier work by not considering this phase sufficiently carefully in this region of the phase diagram. The error was found and corrected as a result of guidance provided by the weak-segregation theory (and by Prof. Erukhimovich).

V. Conclusions

A combination of weak-segregation theory and numerical SCFT theory has been used to flesh out our understanding of the phase behavior of nonfrustrated ABC triblock copolymers.

For the idealized case of completely symmetric systems, with $\chi_{AB} = \chi_{BC}$, we find a line of continuous ODTs within the isopleth $f_A = f_C$ at and near the value $k = 4$ suggested by the Hildebrand approximation, but predominantly first-order ODTs at lower values of k. We have clarified the sequence of ordered phases near the ODT for such symmetric systems. Notably, we have identified a region in which an alternating diamond (D^A) phase is stable near the ODT. In systems with the value of $k = 4$ suggested by the Hildebrand approximation for the χ parameters, we find a phase sequence $D \rightarrow S^A \rightarrow C^A \rightarrow G^A \rightarrow L$ with decreasing f_B in relatively strongly segregated systems, but find that the C^A phase is replaced by a D^A phase in a relatively small region near the ODT.

As an extension of our previous work, we also constructed full composition triangles of two models of more strongly segregated ISO triblock copolymers. We find that the region of stability of the O^{70} phase shrinks with increasing chain length N in a thermodynamically symmetric model, with $\chi_{AC} = \chi_{BC}$, but is enlarged slightly with increasing N in a more realistic, slightly asymmetric model. In both models, the phase diagrams changed surprisingly little when the chain lengths were doubled, except for the replacement of the D^A phase by a C^A phase in more strongly segregated systems. This suggests that the study of systems with experimentally accessible ODTs can provide a useful, but imperfect guide to the equilibrium behavior of higher molecular weight systems, as is also true for diblock copolymers.

With this study, we hope that our qualitative understanding of nonfrustrated ABC triblocks is approaching maturity, though an exhaustive study of the full parameters space remains impractical even for this simple class of systems. Theoretical study of frustrated ABC triblocks remains more difficult, despite recent progress,[11] because of the combination of a large parameter space and a much larger variety of plausible candidate structures.

Acknowledgment. The authors acknowledge a very helpful correspondence with Igor Erukhimovich about the weak-segregation description of what we now call the alternating diamond phase. Resources of the Minnesota Supercomputer Institute were used for the computations presented here. J.Q. received support from NSF Grant DMR-0704192 and from a University of Minnesota Doctoral Dissertation Fellowship.

References and Notes

(1) Nakazawa, H.; Ohta, T. *Macromolecules* **1993**, *26*, 5503–5511.
(2) Zheng, W.; Wang, Z.-G. *Macromolecules* **1995**, *28*, 7215–7223.
(3) Stadler, R.; Auschra, C.; Beckmann, J.; Krappe, U.; Voight-Martin, I.; Leibler, L. *Macromolecules* **1995**, *28*, 3080–3097.
(4) Phan, S.; Fredrickson, G. H. *Macromolecules* **1997**, *31*, 59–63.
(5) Matsen, M. W. *J. Chem. Phys.* **1998**, *108*, 785–796.
(6) Erukhimovich, I. Y.; Abetz, V.; Stadler, R. *Macromolecules* **1997**, *30*, 7435–7443.
(7) Erukhimovich, I. Y. *Eur. Phys. J. E* **2005**, *18*, 383–406.

(8) Tyler, C. A.; Morse, D. C. *Phys. Rev. Lett.* **2005**, *94*, 208302.
(9) Tyler, C. A.; Qin, J.; Bates., F. S.; Morse, D. C. *Macromolecules* **2007**, *40*, 4654–4668.
(10) Sun, M.; Wang, P.; Qiu, F.; Tang, P.; Zhang, H.; Yang, Y. *Phys. Rev. E* **2008**, *77*, 016701.
(11) Guo, Z.; Zhang, G.; Qiu, F.; Zhang, H.; Yang, Y.; Shi, A. *Phys. Rev. Lett.* **2008**, *101*, 028301.
(12) Leibler, L. *Macromolecules* **1980**, *13*, 1602–1617.
(13) Bailey, T. S.; Hardy, C. M.; Epps, T. H.; Bates, F. S. *Macromolecules* **2002**, *35*, 7007–7017.
(14) Epps, T. H.; Cochran, E. W.; Hardy, C. M.; Bailey, T. S.; Waletzko, R. S.; Bates, F. S. *Macromolecules* **2004**, *36*, 2873–2881.
(15) Mogi, Y.; Kotsuji, H.; Kaneko, Y.; Mori, K.; Matsushita, Y.; Noda, I. *Macromolecules* **1992**, *25*, 5408–5411.
(16) Mogi, Y.; Mori, K.; Matsushita, Y.; Noda, I. *Macromolecules* **1992**, *25*, 5412.
(17) Mogi, Y.; Mori, K.; Kotsuji, H.; Matsushita, Y.; Noda, I.; Han, C. C. *Macromolecules* **1993**, *26*, 5169–5173.
(18) Mogi, Y.; Nomura, M.; Kotsuji, H.; Ohnishi, K.; Matsushita, Y.; Noda, L. *Macromolecules* **1994**, *27*, 6755–66760.
(19) Epps, T. H.; Bates, F. S. *Macromolecules* **2006**, *39*, 2676–2682.
(20) Erukhimovich, I. Y. *Polym. Sci. U.S.S.R.* **1982**, *24*, 2223–2232.
(21) Erukhimovich, I. Y. *Polym. Sci. U.S.S.R.* **1982**, *24*, 2232–2241.
(22) Kuchanov, S. *Macromol. Symp.* **2007**, *252*, 76–89.
(23) Ranjan, A.; Morse, D. C. *Phys. Rev. E* **2006**, *74*, 011803.
(24) Wohlgemuth, M.; Yufa, N.; Hoffman, J.; Thomas, E. L. *Macromolecules* **2001**, *34*, 6083–6089.
(25) Tyler, C. A.; Morse, D. C. *Macromolecules* **2003**, *36*, 8184–8188.
(26) Ranjan, A.; Qin, J.; Morse, D. C. *Macromolecules* **2008**, *41*, 942.
(27) Rasmussen, K.; Kalosakas, G. *J. Polym. Sci. Part B* **2002**, *40*, 1777–1783.
(28) Cochran, E. W.; García-Cervera, C. J.; Fredrickson, G. H. *Macromolecules* **2006**, *39*, 2449–2451.
(29) Tyler, C. A.; Morse, D. C. *Macromolecules* **2003**, *36*, 3764–3774.
(30) Qin, J. *Studies of Block Copolymer Melts by Field Theory and Molecular Simulation*, Thesis, University of Minnesota, **2009**.